Int. J. Nonlinear Anal. Appl.
Volume 12, Special Issue, Winter and Spring 2021, 381-398
ISSN: 2008-6822 (electronic)
http://dx.doi.org/10.22075/ijnaa.2021.22932.2435

Topology optimization of elastic structures with the aim of maximizing the buckling load factor using the level set method

Hesam Abhar[a], Ali Ghoddosian[a,*]

[a]Faculty of Mechanical Engineering, Semnan University, Semnan, Iran

(Communicated by Madjid Eshaghi Gordji)

Abstract

This paper presents a study on Topology optimization of continuum structures with the aim of maximizing the lowest buckling load factor. In the structural shape and topology optimization problems, stability and buckling issues are not usually considered therefore in some cases, long and thin members are obtained in optimized configuration that can lead to the instability of structure. In this article level set method with incorporating a fictitious interface energy is applied to find optimal configuration. One of the main problems in traditional continuum structural optimization methods, which are based on the removal or alterations in element density, is the creation of pseudo buckling modes in the optimization process. These pseudo buckling modes should be identified and removed. The level set optimization method, which is grounded on the moving the structure's boundary, has high ability to control topological complexities. Therefore, the idea of using the level set method has led to the elimination of pseudo buckling modes and the resolving of this problem. Derivation of the required speed term in the level set method is complicated and this derivation term for the buckling load factor is the innovation of this research. Numerical examples are illustrated to prove the effectiveness of this method.

Keywords: Level set, Buckling, Topology optimization, stability, pseudo buckling modes.

1. Introduction

Shape and topology optimization of structures is usually done by considering the strength and stiffness of the structure and taking into account conventional objective functions such as minimizing strain energy or structure's mass. If a long and thin member that is in compression becomes unstable, it usually causes large displacements in the structure which leads to the destruction of the entire structure. Recently more research has been done on buckling optimization. Neves et al, considered

*Corresponding author
Email addresses: hesamabhar@semnan.ac.ir (Hesam Abhar), aghoddosian@semnan.ac.ir (Ali Ghoddosian)

Received: March 2021 *Accepted:* June 2021

the stability of continuum structures in topological optimization. They investigated the reinforcement of the structure for increasing overall structural stability. Neves et al, first wrote the strain energy equation of the structure then divided the strain of the structure into two linear and nonlinear parts. By eliminating high-order terms and replacing the stress in the structure with product of the normal stress caused by the buckling load multiplied by the buckling load factor, they obtained a linear value for the critical load of the structure. Then, using first-order methods based on negative gradient, they optimized the structure to the maximum critical load bearing capacity with a limited volume [6]. Neves et al, also expanded their work to optimizing the buckling of micro-structures periodic material which are affected by local buckling in the same cell structure [7]. Xingjun Gao and Haitao used algorithms based on Changing the density of elements as state variables for buckling optimization and a technique that is called "shifting modes" is used for eliminating the pseudo buckling modes [4]. According to this technique, pseudo modes possess two features:

Some pseudo modes have eigenvalues close to zero or much smaller than the actual values.

Large Deformations occur mainly in an area with low density so the sum of modal strain energy in the areas with low density make a major contribution to the total modal strain energy.

Using the first feature and this property that the initial design of the structure has no pseudo mode due to the lack of low density areas, in the whole process of optimization, modes with eigenvalues much less than the first actual value of the previous step are removed and using the second feature and measuring the modal strain energy of low-density parts relative to the overall modal strain energy and the definition of a threshold, real modes are obtained. Loe and Tang maximized the critical buckling load of continuum structures using an optimization method called "moving iso-surface threshold" [10]. Large deformations, instability and buckling in long structures due to small defects in the manufacturing process have created a fascinating field for robust optimization in these structures, one of which has been made by M. Jansen [5]. Jansen used the end-compliance objective function for nonlinear modeling's. The level set optimization is a classic method that define the geometry of structure implicitly and has been developed greatly through recent years. The level set method was initially provided by Osher and Sethian for moving the boundary of the structure under an initial speed function. In the level set method, the boundary location of the structure which is implicitly expressed by a function with one order higher, is in fact the state variable. This boundary is implicitly moved by the level set equation [8]. The level set method in the field of topology and shape optimization of structures was first presented by Sethian and Wiegmann [11]. Later, Wang et al, made the relation between boundary velocity vector and sensitivity as a meaningful link for the level set method [1]. Eller et al, implemented a similar performance for the level set function, which obtained the boundary velocity during the optimization process by an explicit sensitivity analysis through an adjoint method [13]. Qi Xia a, Michael Yu Wang b, and Tielin Shi optimized both topology and support of structures by the level set method, for which in addition to considering variations in the neumann boundary conditions also considered variations in dirichlet boundary conditions. Xia, Wang and Shi also using a move limit strategy for the structure's boundary and prevention of extreme velocity variation, increased the stability and convergence rate of the optimization problem [14]. Takayuki Yamada, Izui, and Takezawa caused an additional term in level set equation by adding a fictitious energy term to the objective function, which is very useful in stability of solving and controlling the complexity of the topology during the optimization process [15]. Peng Wei, Li and Xueping Li and Michael Yu Wang, using radial basis functions, succeeded in developing a new optimization method using level set. in a way that topology variations occur much softer and more stable during the optimization process [12]. Peter D. Dunning et al. considered the buckling constraint into the level set method for the shape optimization of continuum structures [3]. The main focus of Dunning's research is to find sustainable, fast and

accurate solutions in extracting the eigenmodes and the eigenvalues of the structure and there is no explanation of how to extract the term of velocity, which is the complicated and main component of the level set method. Also, because the method used in this research is based on shape optimization rather than topology optimization, the extracted optimized shape is highly dependent on the initial structure and inevitably, some holes are considered for optimization in the initial topology of the its examples. There is also no explanation for the difference in the shape and topology of the optimized structure before applying buckling constraint and thereafter. In this research by derivation of the required velocity term in order to using in topology optimization instead of shape optimization and using the newer and more sustainable level set method, the dependency on the initial topology of the optimization problem is completely eliminated. The derivation of the required velocity term in level set method for maximizing the first critical buckling load factor is the innovation of this research.

2. The topology optimization with level set method

Based on explanation in [15], the level set function in optimization problem is defined as follows:

$$\begin{cases} 0 < \Phi(x) \leq 1 & \forall x \in \Omega \setminus \partial\Omega \\ \Phi(x) = 0 & \forall x \in \partial\Omega \\ -1 \leq \Phi(x) < 0 & \forall x \in D \setminus \partial\Omega \end{cases} \tag{1}$$

The value of level set function, in the far enough distances from structure's boundary is considered to be equal 1 or -1. The topology optimization problem is defined to minimize the objective function, F, on the fixed design domain, D. Fixed design domain consists of solid material domain, Ω, which is $\Omega \subset D$ and complementary void domain, $D \setminus \Omega$. The optimization problem can be stated as

$$\min_{\chi\Omega} F(\chi_\phi(\phi)) = \int_D f(X)\chi_\phi(\phi)d\Omega \tag{2}$$

$$G(\chi_\phi(\phi)) = \int_D \chi_\phi(\phi)d\Omega - V_{max} < 0 \tag{3}$$

$$\chi_\phi(\phi) = \begin{cases} 1 & if\ \phi(x) \geq 0 \\ 0 & if\ \phi(x) < 0 \end{cases} \tag{4}$$

X are points located in Ω that represent the state variables. The G function is volume constraint and V_{max} is the upper limit of the required volume for optimized topology. The characteristic function, $\chi_\phi(\phi)$ is defined in order to expand the problem in the whole fixed design domain D.

The optimization problem is replaced with an unconstrained problem, using Lagrange's method of undetermined multipliers also with adding a fictitious energy term to optimization objective function, it is possible to get an objective function with regularizing ability.

$$\begin{aligned} \min_{\phi} \bar{F}_R(\chi_\phi(\phi), \phi) &= \int_D f(X)\chi_\Phi(\phi)d\Omega + \alpha\left(\int_D \chi_\Phi(\phi)d\Omega - V_{max}\right) + \int_D \tau|\nabla\Phi|^2 d\Omega \\ &= \int_D \bar{f}(X)\chi_\Phi(\phi)d\Omega - \alpha V_{max} + \frac{1}{2}\int_D \tau|\nabla\phi|^2 d\Omega \end{aligned} \tag{5}$$

$barF_R$ is the adjustable objective function and $\tau > 0$ the adjustment parameter which determines the ratio of the initial objective function to fictitious energy term. By setting this parameter, topology complexities created in the optimization solving process can be adjusted conveniently and the inconsistencies due to such complexities are confronted and the process of reaching an optimized topology occurs in a smoother way. α is the Lagrange multiplier and we have $\bar{f} = f + \alpha$.

Based on the KKT conditions the optimization problem is explained as bellow:

$$\langle \frac{d\bar{F}_R\Big(\chi_\phi(\phi)\Big)}{d\phi}, \Phi \rangle = 0 \quad , \quad \alpha G = 0 \quad , \quad \alpha \geq 0 \quad , \quad G \leq 0 \tag{6}$$

Where the notation $\langle \frac{d\bar{F}_R}{d\phi}, \Phi \rangle$ represents the Frèchet derivative of the regularized Lagrangian $\bar{F}_R$ with respect to ϕ in the direction of Φ.

The level set functions which can satisfy conditions (6), are the answers of the optimization problem. But finding such solution directly is almost impossible, thus level set equation is defined as a time evolution equation with fictitious variable t. For making a time evolution equation it is assumed that variations of level set function relative to time t equals the negative gradient of the objective function which $K > 0$ is the coefficient of proportionality.

$$\frac{d\phi}{\partial t} = -K \ \frac{d\bar{F}_R}{d\phi} \tag{7}$$

By replacing of equation (5) into (7) we have:

$$\frac{d\phi}{\partial t} = -K \ (\frac{d\bar{F}}{d\phi} - \tau \nabla^2 \phi) \tag{8}$$

$\frac{d\bar{F}}{D\phi}$ is topological derivative function and equals required velocity term in level set that is described as follows:

$$d_t \bar{F} = \lim_{\varepsilon \to 0} \frac{\bar{F} + \partial \bar{F}}{meas(\Omega \setminus \Omega_\varepsilon) - meas(\Omega)} \tag{9}$$

As shown in Fig. 1, the topological derivative concept means variation of objective function when a hole Ω_ε with small radius ε is created in a specific point of material domain Ω. Γ_ε specifies the boundary of the hole.

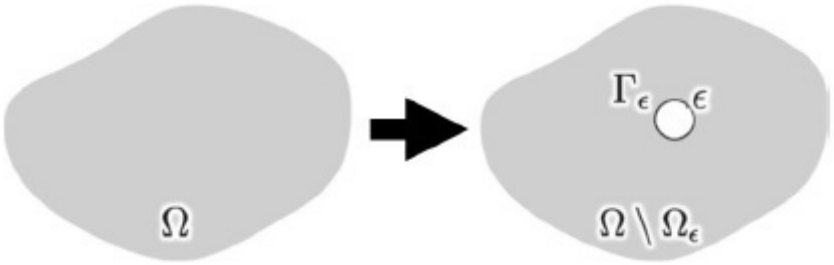

Fig. 1. Topological derivative concept

The time evolution equation is ultimately defined as bellow:

$$\begin{cases} \frac{d\phi}{\partial t} = -K \ (\frac{d\bar{F}}{d\phi} - \tau \nabla^2 \phi) & in \ \ D \\ \phi = 0 & on \ \partial D \end{cases} \tag{10}$$

The above equation is a reaction-diffusion equation which by adjusting the suitable amount for τ the solving complexities can be controlled.

The time derivative of $\bar{F}_R$ function using equation (5) and (10) is as follows:

$$\frac{d\bar{F}}{dt} = \int_D \frac{d\bar{F}_R}{d\phi} \ \frac{\partial \phi}{\partial t} dD = \int_D \frac{d\bar{F}_R}{d\phi} \Big(- K \frac{d\bar{F}_R}{d\phi} \Big) dD = - \int_D K \Big(\frac{d\bar{F}_R}{d\phi} \Big)^2 dD \leq .0 \tag{11}$$

The above equation implies the fact that the sum of the original Lagrangian $\bar{F}$ and the fictitious interface energy decreases monotonically when the level set function is updated based on Eq. (11),

3. The buckling optimization problem definition

The optimization problem is defined as maximizing the first critical buckling load factor or minimizing the negative first critical buckling load factor. Also, the required volume constraint and structural equilibrium equations for a plain stress problem must be satisfied.

$$min\ F = \lambda_{cr} \tag{12}$$

$$\begin{cases} -div(\mathcal{C}_{ijkl}\ e_{k,l}(u)) = 0 & on\ \Omega \\ u_i = \bar{u}_i & on\ \Gamma_u \\ t_i = \bar{t}_i & on\ \Gamma_t \end{cases} \tag{13}$$

$$G = \int_\Omega d\Omega - V_{max} leq 0 on\ \Omega \tag{14}$$

λ_{cr} is the first critical buckling load factor, $\mathcal{C}_{ijkl}$ is the elasticity tensor, t_i or traction is equal $\sigma_{ij}n_j$ and equal $\mathcal{C}_{ijkl}\ u_{k,l}\ n_j$; Also, $\bar{u}_i$ and $\bar{t}_i$ are the constant values for displacement and traction in the boundary of Γ_u and Γ_t, respectively.

The critical load factor is defined as bellow [2].

$$\int_\Omega \mathcal{C}_{ijkl}\ e_{i,j}(\psi)\ e_{k,l}(\phi)d\Omega + \lambda \int_\Omega \mathcal{C}_{ijkl}\ e_{k,l}(u)\psi_{m,i}\Phi_{m,j}d\Omega = 0$$

$$OR \quad \lambda = -\frac{\int_\Omega \mathcal{C}_{ijkl}\ e_{i,j}(\psi)\ e_{k,l}(\phi)d\Omega}{\int_\Omega \mathcal{C}_{ijkl}\ e_{k,l}(u)\psi_{m,i}\varphi_{m,j}d\Omega} \tag{15}$$

ψ is the structure's mode shape of buckling and e is the strain.

In order to replace the constrained problem with an unconstrained problem, $\bar{F}$, the Lagrange's method of undetermined multipliers is used with Lagrange multipliers of α and $\tilde{u}$:

$$\bar{F} = -\lambda_{cr} + \int_\Omega \tilde{u}_i div(\mathcal{C}_{ijkl}\ e_{k,l}(u))d\Omega + \alpha(\int_\Omega d\Omega - V_{\max}). \tag{16}$$

The second term on the right-hand side of the above equation is replaced, using Green's formula as follows:

$$\bar{F} = -\lambda_{cr} + \int_\Gamma \tilde{u}_i t_i d\Gamma - \int_\Omega \mathcal{C}_{ijkl}\ e_{k,l}(u)d\Omega + \alpha(\int_\Omega d\Omega - V_{\max}). \tag{17}$$

There is a need to calculate $\partial\bar{F}$ for determination of topological derivative. For this reason, with creating an enough small hole in the material domain Ω and using introduced method of [9], equilibrium equation (15-18) can be described as:

$$\begin{array}{ll} Div(C_{ijkl}\ (e_{k,l}(u) + \delta e_{k,l}(u))) = 0 & in\ \Omega \setminus \Omega_\varepsilon \\ u_i + \delta u_i = \bar{u}_i & in\ \Gamma_u \\ t_i + \delta t_i = \bar{t}_i & in\ \Gamma_t \\ t_i + \delta t_i = 0 & in\ \Gamma_\varepsilon. \end{array}$$

And it is assumed that the new equilibrium equation of the structure satisfies the former boundary condition and no traction would be applied on the boundaries of the created hole. So for finding $\delta\bar{F}$ first of all $\delta\lambda_{cr}$ should be calculated. The Lagrangian of equation (15) that includes the created hole

for critical load factor is given as:

$$\begin{aligned}\int_{\Omega\setminus\Omega_\varepsilon} \mathcal{C}_{ijkl}\ e_{i,j}(\psi)\ e_{k,l}(\phi)d\Omega \ &+\ \delta\lambda_{cr}\int_{\Omega} \mathcal{C}_{ijkl}\ e_{k,l}(u)\psi_{m,i}\varphi_{m,j}d\Omega \\ &+\ \lambda_{cr}\int_{\Omega\setminus\Omega_\varepsilon} \mathcal{C}_{ijkl}\ \delta e_{k,l}(u)\psi_{m,i}\varphi_{m,j}d\Omega \\ &+\ \lambda_{cr}\int_{\Omega\setminus\Omega_\varepsilon} \mathcal{C}_{ijkl}\ e_{k,l}(u)\psi_{m,i}\varphi_{m,j}d\Omega = 0 \end{aligned} \tag{22}$$

With subtracting above equation from (15):

$$\begin{aligned}-\int_{\Omega_\varepsilon} \mathcal{C}_{ijkl}\ e_{i,j}(\psi)\ e_{k,l}(\varphi)d\Omega \ &+\ \delta\lambda_{cr}\int_{\Omega} \mathcal{C}_{ijkl}\ e_{k,l}(u)\psi_{m,i}\varphi_{m,j}d\Omega \\ &+\ \lambda_{cr}\int_{\Omega\setminus\Omega_\varepsilon} \mathcal{C}_{ijkl}\ \delta e_{k,l}(u)\psi_{m,i}\varphi_{m,j}d\Omega \\ &-\ \lambda_{cr}\int_{\Omega_\varepsilon} \mathcal{C}_{ijkl}\ e_{k,l}(u)\psi_{m,i}\varphi_{m,j}d\Omega = 0. \end{aligned} \tag{23}$$

And considering this fact that $\int_{\Omega_\varepsilon} \mathcal{C}_{ijkl}\ e_{i,j}(\psi)\ e_{k,l}(\phi)d\Omega + \lambda_{cr}\int_{\Omega} \mathcal{C}_{ijkl}\ e_{k,l}(u)\psi_{m,i}\varphi_{m,j}d\Omega$ is also equal zero, $\delta\lambda_{cr}$ is achieved as follows:

$$\delta\lambda_{cr} = -\lambda_{cr}\frac{\int_{\Omega\setminus\Omega_\varepsilon} \mathcal{C}_{ijkl}\ \delta e_{k,l}(u)\psi_{m,i}\varphi_{m,j}d\Omega}{\int_{\Omega} \mathcal{C}_{ijkl}\ e_{k,l}(u)\psi_{m,i}\varphi_{m,j}d\Omega}. \tag{24}$$

Therefore:

$$\begin{aligned}\bar{F}+\delta\bar{F} \ &=\ -\lambda_{cr} - \delta\lambda_{cr} + \int_{\Gamma_u U\Gamma_t} \tilde{u}_i(t_i+\delta t_i)d\Gamma + \int_{\Gamma_\varepsilon} \tilde{u}_i(t_i+\delta t_i)d\Gamma \\ &\quad -\int_{\Omega\setminus\Omega_\varepsilon} e_{i,j}(\tilde{u})\ \mathcal{C}_{ijkl}(u_{k,l}+\delta u_{k,l}d\Omega + \alpha(\int_{\Omega\setminus\Omega_\varepsilon} d\Omega - V_{\max}). \end{aligned} \tag{25}$$

$$\begin{aligned}\bar{F}+\delta\bar{F} \ &=\ -\lambda_{cr} + \lambda_{cr}\ \frac{\int_{\Omega\setminus\Omega_\varepsilon} \mathcal{C}_{ijkl}\ \delta e_{k,l}(u)\psi_{m,i}\varphi_{m,j}d\Omega}{\int_{\Omega} \mathcal{C}_{ijkl}\ e_{k,l}(u)\psi_{m,i}\varphi_{m,j}d\Omega} + \int_{\Gamma_u U\Gamma_t} \tilde{u}_i(t_i+\delta t_i)d\Gamma \\ &\quad +\int_{\Gamma_\varepsilon} \tilde{u}_i(t_i+\delta t_i)d\Gamma - \int_{\Omega\setminus\Omega_\varepsilon} e_{i,j}(\tilde{u})\ \mathcal{C}_{ijkl}(u_{k,l}+\delta u_{k,l}d\Omega + \alpha(\int_{\Omega\setminus\Omega_\varepsilon} d\Omega - V_{\max}). \end{aligned}$$

With the replacement of equation (21) in the fourth term of the above equation, this term will be omitted. Also, by normalizing eigenvectors related to stress stiffness matrix, in fact, denominator will be reduced to one. Furthermore, with subtracting Eq (25) from Eq. (17), $\delta\bar{F}$ would be as follows:

$$\begin{aligned}\delta\bar{F} \ &=\ \lambda_{cr}\int_{\Omega\setminus\Omega_\varepsilon} \mathcal{C}_{ijkl}\ \delta e_{k,l}(u)\psi_{m,i}\psi_{m,j}d\Omega - \lambda_{cr}\int_{\Omega_\varepsilon} \mathcal{C}_{ijkl}\ e_{k,l}(u)\psi_{m,i}\psi_{m,j}d\Omega \\ &\quad +\int_{\Gamma_u U\Gamma_t} \tilde{u}_i\delta t_i d\Gamma - \int_{\Omega\setminus\Omega_\varepsilon} \tilde{u}_{i,j}\ \mathcal{C}_{ijkl}\delta e_{k,l}(u)d\Omega + \int_{\Omega_\varepsilon} e_{i,j}(\tilde{u})\mathcal{C}_{ijkl}\delta e_{k,l}(u)d\Omega \\ &\quad -\alpha\int_{\Omega_\varepsilon} d\Omega. \end{aligned} \tag{26}$$

The second and the fifth term on the right-hand side of the above equation can be replaced, using Green's formula as follows:

$$\begin{aligned}&\int_{\Omega\setminus\Omega_\varepsilon} \mathcal{C}_{ijkl}\ \delta e_{k,l}(u)\psi_{m,i}\psi_{m,j}d\Omega\\&\quad=\int_{\Gamma_t}\mathcal{C}_{ijkl}\ \psi_{m,i}\psi_{m,j}n_l\delta u_k d\Gamma+\int_{\Gamma_\varepsilon}\mathcal{C}_{ijkl}\ \psi_{m,i}\psi_{m,j}n_l\delta u_k d\Gamma\\&\qquad-\int_{\Omega\setminus\Omega_\varepsilon} div(\mathcal{C}_{ijkl}\psi_{m,i}\psi_{m,j})\delta u_i d\Omega,\end{aligned}\tag{27}$$

and

$$\begin{aligned}&\int_{\Omega\setminus\Omega_\varepsilon} e_{i,j}(\tilde{u})\ \mathcal{C}_{ijkl}\delta e_{k,l}(u)d\Omega\\&\quad=\int_{\Gamma_u U\Gamma_t}\tilde{t}_i\delta u_i d\Gamma+\int_{\Gamma_\varepsilon}\mathcal{C}_{ijkl}e_{i,j}(\tilde{u})n_l\delta u_k d\Gamma\\&\qquad-\int_{\Omega\setminus\Omega_\varepsilon} div(\mathcal{C}_{ijkl}e_{i,j}(\tilde{u}))\delta u_i d\Omega.\end{aligned}\tag{28}$$

With replacing Eq. (27) and (28) into Eq. (26) and considering that the boundary conditions wouldn't change before and after the creation of the hole, that's mean: $\begin{array}{ll}\delta u_i=0 & on\ \Gamma_u\\ \delta t_i=0 & on\ \Gamma_t.\end{array}$

Then the result will be:

$$\begin{aligned}\delta\bar{F}\ &=\ \lambda\Bigg(\int_{\Gamma_t}\mathcal{C}_{ijkl}\ \psi_{m,i}\psi_{m,j}n_l\delta u_k d\Gamma+\int_{\Gamma_\varepsilon}\mathcal{C}_{ijkl}\ \psi_{m,i}\psi_{m,j}n_l\delta u_k d\Gamma\\&\quad-\int_{\Omega\setminus\Omega_\varepsilon} div(\mathcal{C}_{ijkl}\psi_{m,i}\psi_{m,j})\delta u_i d\Omega\Bigg)+\int_{\Omega\setminus\Omega_\varepsilon} div(\mathcal{C}_{ijkl}e_{i,j}(\tilde{u}))\delta u_i d\Omega\\&\quad-\int_{\Gamma_t}\tilde{t}_i\delta u_i d\Gamma+\int_{\Gamma_u}\tilde{u}_i\delta t_i d\Gamma+\int_{\Omega_\varepsilon}e_{i,j}(\tilde{u})\mathcal{C}_{ijkl}\delta e_{k,l}(u)d\Omega\\&\quad-\int_{\Gamma_\varepsilon}\mathcal{C}_{ijkl}e_{i,j}(\tilde{u})n_l\delta u_k d\Gamma-\alpha\int_{\Omega_\varepsilon}d\Omega.\end{aligned}\tag{31}$$

If all integral coefficients that include δu_i and δt_i are canceled out, the adjoint equation will be defined as follows:

$$div(\mathcal{C}_{ijkl}e_{i,j}(\tilde{u}))=\lambda div(\mathcal{C}_{ijkl}\psi_{m,i}\psi_{m,j})\quad in\ \Omega\tag{32}$$

$$\tilde{u}_i=0\quad on\ \Gamma_u\tag{33}$$

$$\tilde{t}_i=\lambda\ \mathcal{C}_{ijkl}\psi_{m,i}\psi_{m,j}n_l\quad on\ \Gamma_t.\tag{34}$$

Then $\tilde{u}$ or Lagrange multiplier of the adjoint equation is obtained by solving the above equation. As the result, $\delta\bar{F}$ will be equal to:

$$\begin{aligned}\delta\bar{F}\ &=\ \lambda\int_{\Gamma_t}\mathcal{C}_{ijkl}\ \psi_{m,i}\psi_{m,j}n_l\delta u_k d\Gamma+\int_{\Omega_\varepsilon}e_{i,j}(\tilde{u})\mathcal{C}_{ijkl}\delta e_{k,l}(u)d\Omega\\&\quad-\int_{\Gamma_\varepsilon}\mathcal{C}_{ijkl}e_{i,j}(\tilde{u})n_l\delta u_k d\Gamma-\alpha\int_{\Omega_\varepsilon}d\Omega.\end{aligned}\tag{35}$$

In the above equation, δu is still unknown. In order to obtain δu , the boundary value problem (18-21) is subtracted from boundary value problem (13) and result is as follows:

$$
\begin{aligned}
&div(\mathcal{C}_{ijkl}\delta u_{k,l}) = 0 \quad in\ \Omega \setminus \Omega_\varepsilon && (36)\\
&\delta u_i = 0 \quad on\ \Gamma_u && (37)\\
&\delta t_i = 0 \quad on\ \Gamma_t && (38)\\
&\delta t_i = -t_i \quad on\ \Gamma_\varepsilon && (39)
\end{aligned}
$$

In the above problem, because the radius of the hole ε is considered small enough, the effect of Γ_u and Γ_t boundaries can be ignored for solving δu_i on Γ_ε, so that the above problem is transformed to the boundary value problem as bellow:

$$
\begin{aligned}
&div(\mathcal{C}_{ijkl}\delta u_{k,l}) = 0 \quad in\ \Omega \setminus \Omega_\varepsilon && (40)\\
&\delta t_i = -\sigma^{\circ}_{i,j}\ n_j + O(\varepsilon) \quad on\ \Gamma_\varepsilon && (41)
\end{aligned}
$$

That the 0 denotes the situation before creating the hole. This equation is solved by Guzina and Bonnet in 2004 [14] and result for sphere Γ_ε is as follows:

$$
\delta u_i = -\frac{\varepsilon}{\mu}\left(\frac{4-5\nu}{7-5\nu}\ \sigma^{\circ}_{i,j}\ n_j - \frac{3-5\nu}{4(7-5\nu)}\ \sigma^{\circ}_{i,j}\ n_j\right) + O(\varepsilon) \tag{42}
$$

After replacement of $\delta\bar{F}$ in topological derivative formula (9) and getting the limit, it will be:

$$
d_t\bar{F} = \lim_{\varepsilon\to 0}\ \frac{\delta\bar{F}}{\frac{4\pi\varepsilon^3}{3}} = e_{i,j}(\tilde{u})\ \mathcal{A}_{ijkl}\ u^{\circ}_{k,l} - \lambda\ u^{\circ}_{k,l}\ \mathcal{B}_{ijkl}\ \psi^{\circ}_{m,i}\psi^{\circ}_{m,j} - \alpha. \tag{43}
$$

That $\mathcal{A}$ is equal to:

$$
\begin{aligned}
\mathcal{A}_{ijkl} &:= \mathcal{A}_1\ \delta_{ij}\ \delta_{kl} + \mathcal{A}_2(\delta_{ik}\ \delta_{jl} + \delta_{il}\ \delta_{jk})\\
\mathcal{A}_1 &= -\frac{3(1-\nu)(1-14\nu+15\nu^2)}{2(1+\nu)(7-5\nu)(1-2\nu)^2}\ E\\
\mathcal{A}_2 &= \frac{15E(1-\nu)}{2(1+\nu)(7-5\nu)}.
\end{aligned} \tag{44}
$$

And $\mathcal{B}$ is equal to:

$$
\begin{aligned}
\mathcal{B}_{ijkl} &:= \mathcal{B}_1\ \delta_{ij}\ \delta_{kl} + \mathcal{B}_2(\delta_{ik}\ \delta_{jl} + \delta_{il}\ \delta_{jk})\\
\mathcal{B}_1 &= -\left[\frac{4-5\nu}{7-5\nu}\ \frac{3\lambda^2+4\mu\lambda}{\mu} - \frac{3-5\nu}{4(7-5\nu)}\ \frac{(3\lambda+2\mu)^2}{\mu}\right],\\
\mathcal{B}_2 &= 2\ \frac{4-5\nu}{7-5\nu}.
\end{aligned} \tag{45}
$$

4. Simulation

4.1. The finite element analysis

To solve the boundary value problems, it is used to getting conventional finite element method. However, this method contains a major issue. With choosing the nodal design variable, checkerboard patterns are avoided but a layering or is landing phenomenon of black and white regions in the design domain may appear. For avoiding this phenomenon, a hybrid stress finite element method is used in this approach [4]. Because of using the independent shape functions in the calculation of stress

components in this method, the spectrum stress is smoother and some high-level and parasitic stresses which are caused by small irregular and sharp edges eliminate. In this method in order to define the displacement of $\mathbf{u}$ and the stress of σ , further relations are used.

Following the optimization process, eigenvalues and eigenvectors are attainable through the bellow formula:

$$K + \lambda_j K_G \psi_j = 0 \tag{46}$$

K and K_G are stiffness, stress stiffness tensors and λ_j, ψ_j are eigenvalues and eigenvectors respectively.

4.2. Solving the buckling problem example

To make sure if the coding of hybrid stress finite element method is valid, the first critical load factor of a "One fixed end-one pinned end" column is calculated and compared with Euler's formula, $P_{cr} = \dfrac{\pi^2 EI}{(Le)^2}$(?^{2} , the effective length of a column with one fixed end and one pin-connected end is $L_e = 0.699L \approx 0.7L$. With taking 100 as column length, L, 6 for width and 10 for thickness and also Young modulus $E = 1$, the theoretical first critical load factor is equal to:

$$P_{cr} = \frac{\pi^2 EI}{(Le)^2} = 0.36 \tag{47}$$

In the simulation $\lambda_{cr} = 0.36$ is obtained by putting the applied downward concentrated load value equal to 1. As it is obvious, the results are in exact agreement with each other and indicate the correctness of the simulation. Fig. 2 shows the first eigenmode of the column.

Fig. 2. The First eigenmode shape

5. Numerical examples

Example 5.1. *The first example is a 2D "One fixed end" column under a downward uniform distributed load which is shown in Fig.3. With* 24×40*-dimensions, Young's modulus* $E = 1$*, Poisson's ratio* $\nu = 0.3$ *and unit thickness. The design domain is discretized into* 24×40 *equally-sized square four-node plain stress elements. Distributed load* $q = 0.01$ *is applied and the section of the applied load is one seventh of middle width of column and applied load is uniform. The maximum required*

volume fraction is set to 0.4. *The regulation parameter* $\tau = 0.001$ *and fictitious time increment* $\Delta t = 0.01$ *are considered for solving the level set equation. In order to avoid from numerical errors, the Young's modulus is set to* $10^{(} - 6)$ *for the elements outside of the design domain. Simulation is converged after about* 160 *iterations and the resulted first critical buckling load factor equals* 9.9. *The optimized topology is shown in Fig. 4.*

Fig. 3. One fixed end continuum structure under distributed load

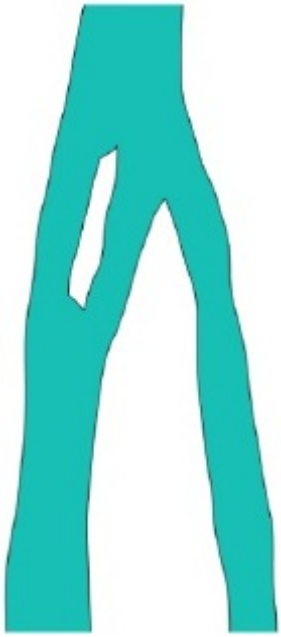

Fig. 4. Optimized Topology

As it is noticeable in Fig. 4, the optimized topology is formed by two open arms ($\bigwedge$ *shape), and buckling is prevented although the volume of the structure reduces to* 40% *of the initial volume. The process of change in the volume fraction and buckling load factor are shown in Fig. 5 and 6, respec-*

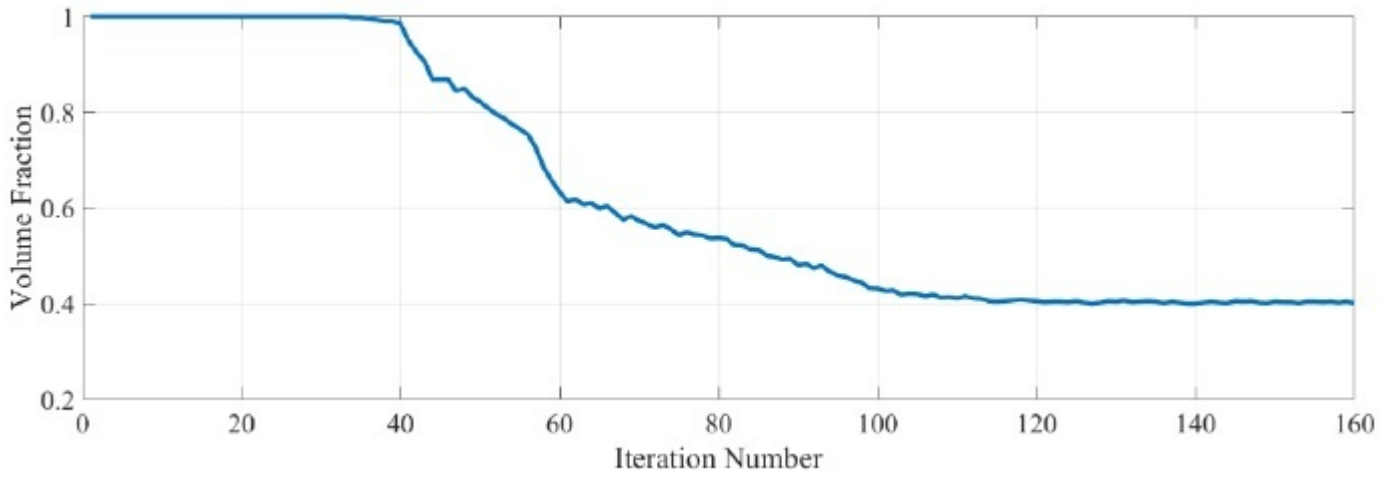

tively.

Fig. 5. Changes in the volume fraction

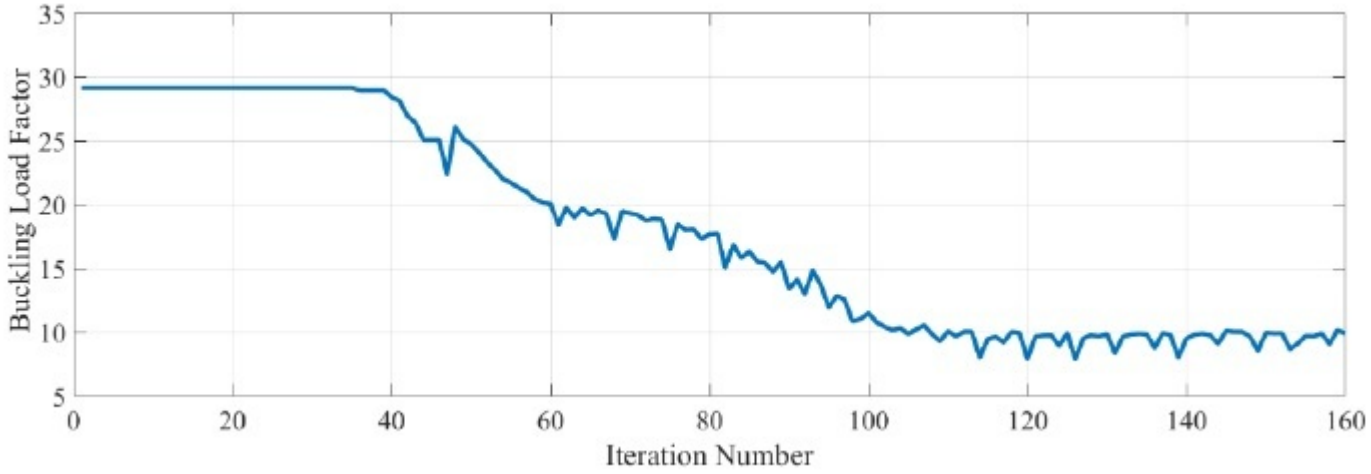

Fig. 6. Changes in the buckling load factor

In Fig. 7 the gradual process of getting to optimized topology is shown.

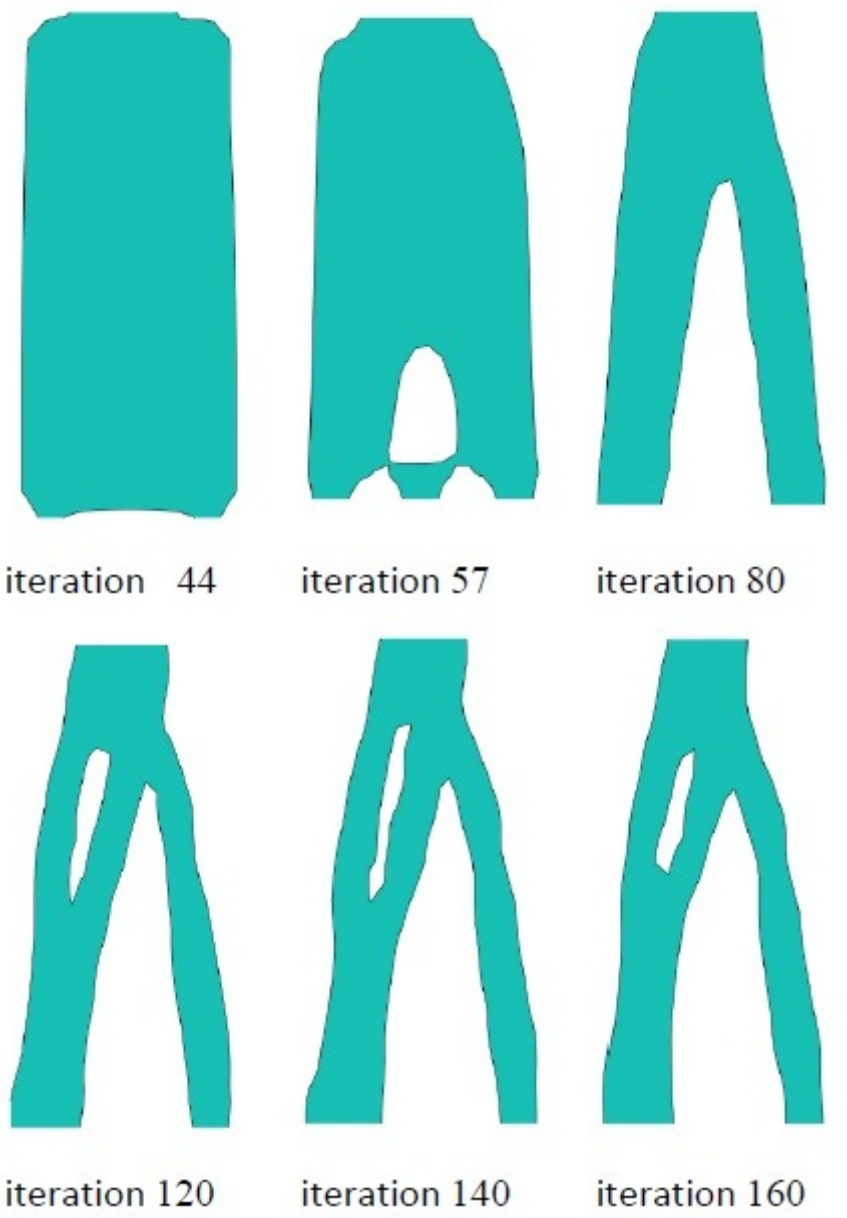

Fig. 7. Gradual Changes of Optimization

The possibility of buckling and instability exists only in the members of optimized topology that are in exposure to compressive load (members in compression). Due to the nature of asymmetrical buckling, even the concentrated or distributed load is precisely applied in the middle of the initial symmetric column (Fig. 2), the optimization process continues in a way that the members in compression get wider than corresponding members, which are in tensile. This phenomenon ends up in the creation of an antisymmetric optimized topology. With a minor movement of applied load to right or left, relative to the longitudinal line center of the column (eccentric load), The location of the members in compression is changed with members in tensile and vice versa instantly that is a justification for all that is said (Fig. 8).

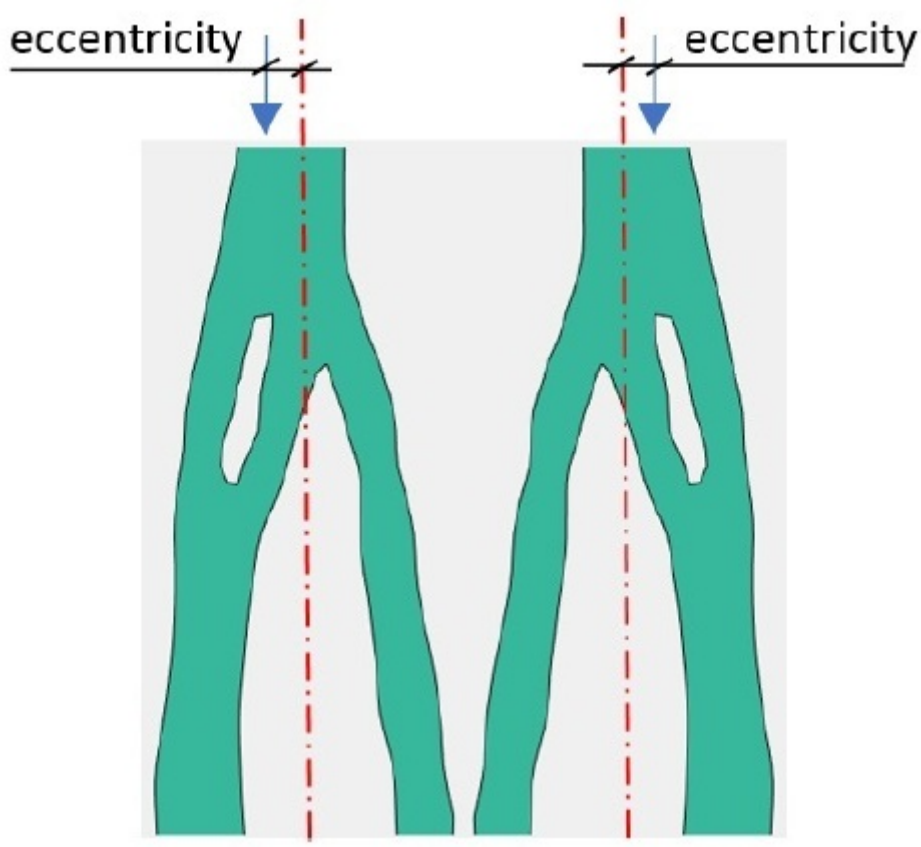

Fig. 8: Change the location of members in compression and tensile due to the movement of the load location

Example 5.2. *The initial shape, supports, applied load, material properties, element type and volume constraint of this example are similar to the second example of the article [4] that use The SIMP (Solid Isotropic Material with Penalization) method for optimization. This example is a short cantilever beam under a concentrated load which is shown in Fig. 9. With* 1×2*-dimensions, Young's modulus* $E = 1$*, Poisson's ratio* $\nu = 0.3$ *and unit thickness. The design domain is discretized into* 30×60 *equally-sized square four-node plain stress elements.*

The downward concentrated load $F = 0.005$ *is applied to the center of the right edge. The maximum required volume fraction is set to* 0.15*. The regulation parameter* $\tau = 0.001$ *and fictitious time increment* $\Delta t = 0.01$ *for solving the level set problem are considered.*

Firstly, this example is solved for a conventional minimum compliance and the optimized topology is shown in Fig. 10(a) and the corresponding first buckling load factor is equal to 0.22 *that is precisely equal with mentioned example of the article [4] Fig. 10(b).*

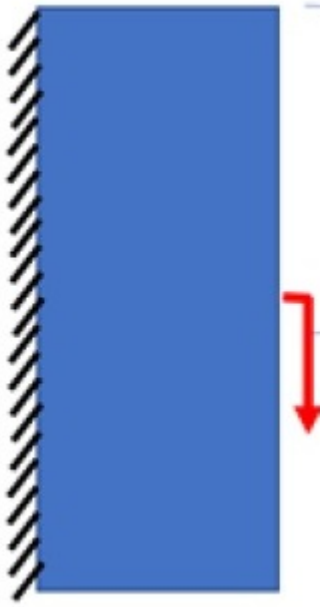

Fig. 9. One fixed end continuum structure under concentrated load.

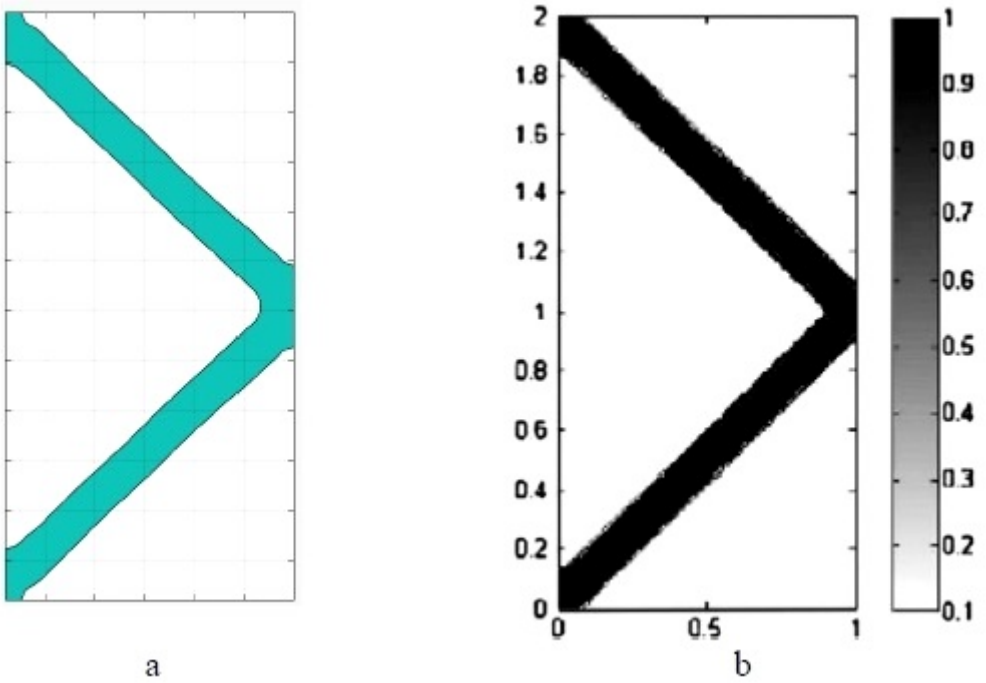

Fig. 10. Optimized topology of minimum compliance. a) level set, b) SIMP method [3]

Next, the simulation is done with the first critical buckling load factor as objective function and consideration of two different values of 0.001 *and* 0.01 *for adjustment parameter* τ.

In the first simulation, because of relatively small values of $\tau = 0.001$, *the optimization process suffers from instability of the solution due to the creation of pseudo modes yields divergence and cessation of the optimization process. Divergent simulation result is shown in Fig. 11.*

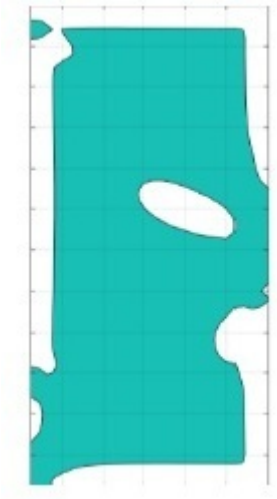

Fig. 11. Divergent simulation process.

Based on Fig. 12, it is clear in the 34th iteration of the optimization process, a very small pseudo eigenvalue with greatly deviation from the other normal eigenvalues, leads to instability of the solution and further divergence of the problem.

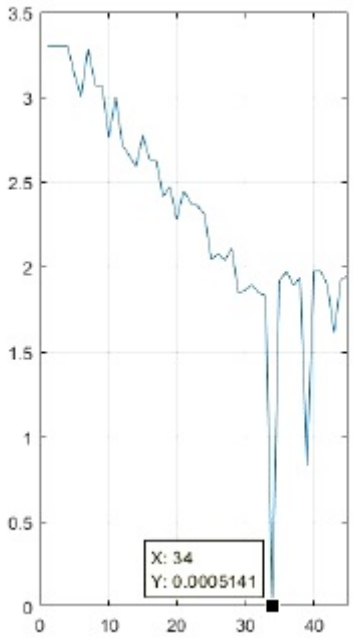

Fig. 12. The first critical buckling load factor of optimization during optimization process and creation of a very small pseudo eigenvalue in the 34th iteration.

In the second simulation with $\tau = 0.01$*, the simulation is converged After 150 iterations and optimized topology is shown in Fig.13(a). Because of using the first critical buckling load factor instead of minimum compliance, the corresponding first critical buckling load factor is higher and equal to* 0.4 *that shown in Fig. 14 and the final volume of the structure according to Fig. 15 is exactly* 15% *of the initial volume. Also, this example has been compared with the second example of the article [4] for validation of the results. The article [4] uses SIMP (Solid Isotropic Material with Penalization) method for optimization via 3 different algorithms and results shown in Fig. 13(b, c, d). It is obvious that in both methods the lower arm of the optimized topology which is in compression,*

tries to become wider than the upper arm that is in tensile and in the one of SIMP algorithms lower arm tries to get shorter with shifting upward like level set algorithm. Although the level set optimization process is simulated with less element discretizing in comparison with the second example of the article [4] (30×60 *versus* 40×80*), the results are approximately similar. Also using the level set method completely solves the main problem of the gray elements mentioned in the second example of the article [4] and the structural boundaries are quite clear.*

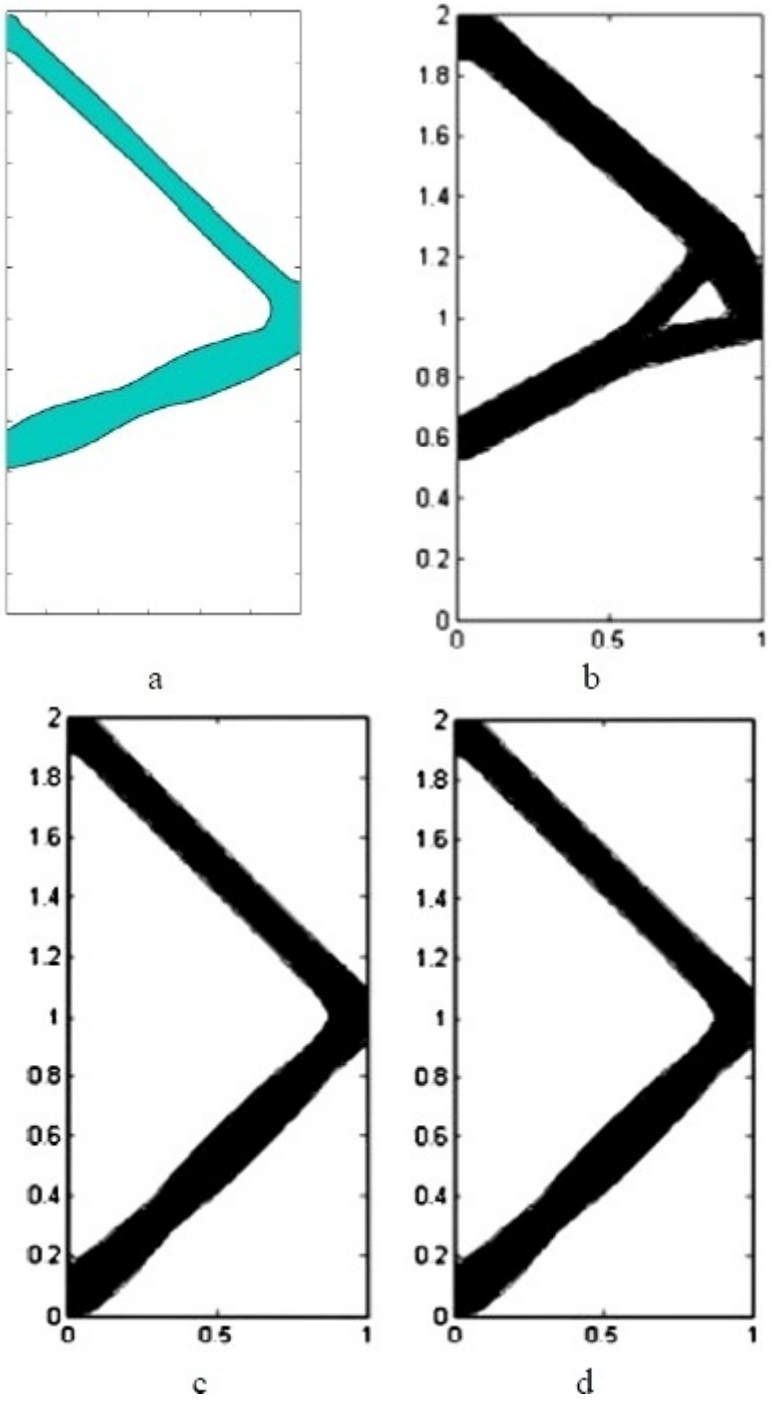

Fig. 13. Optimized topology a) level set and b, c, d) different SIMP algorithm methods [3]

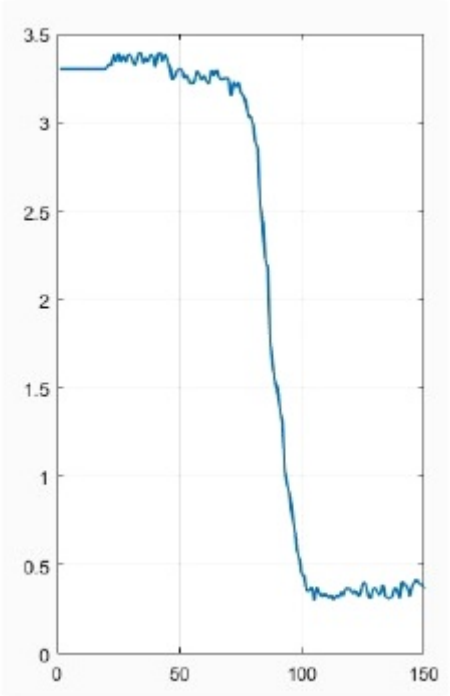

Fig. 14. Changes in the first critical buckling load factor during optimization process

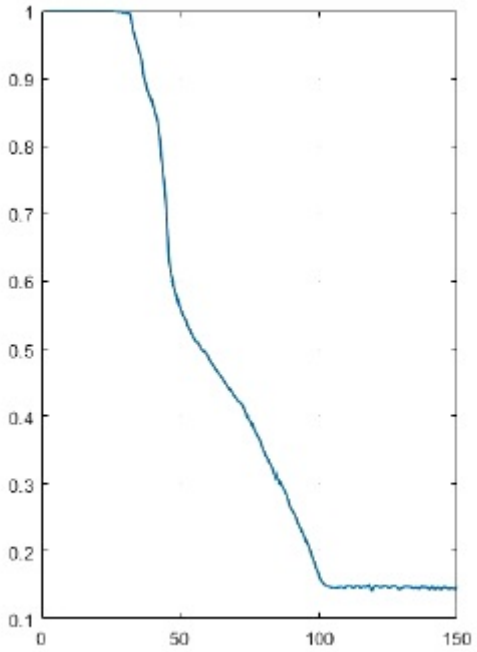

Fig. 15. Changes in the ratio of the required volume of the structure to the initial volume during optimization process

6. Conclusion

In this study, the problem of buckling stability for two-dimensional continuous structures is investigated. The optimization problem was solved by level set method and the optimal topology was obtained independently from the initial topology. Also, the required velocity term in level set equation was calculated using the method of adjoint equations. The main feature of optimal topologies is

having the smaller and wider compression members in compression in the optimized structure. Using the level set optimization method and regulating of adjustment parameter τ, the problem associated with creation of pseudo buckling modes in the conventional methods of optimizing continuum structures has been completely eliminated, and the efficiency of this method are demonstrated through several examples.

Acknowledgements

The authors would like to acknowledge the support from Golgohar Mining and Industrial Co., Sirjan, Iran.

References

[1] G. Allaire, F. Jouve and A.M. Toader, *Structural optimization using sensitivity analysis and a level-set method*, J. Comput. Phys. 194(1) (2004) 363–393.
[2] H.C. Cheng, K.N. Chiang and T.Y. Chen, *Optimal configuration design of elastic structures for stability*, Int. Conf. High Perf. Comput. Asia-Pacific Region, 2002.
[3] P. D. Dunning, E. Ovtchinnikov, J. Scott and H. Alicia Kim, *Level-set topology optimization with many linear buckling constraints using an efficient and robust eigensolver*, Int. J. Numerical Meth. Engin. 10(12)7 (2016) 1029–1053.
[4] X. Gao and H. Ma, *Topology optimization of continuum structures under buckling constraints* Comput. Struct. 157(C) (2015) 142-152.
[5] M. Jansena, G. Lombaerta and M. Schevenelsb, *Robust topology optimization of structures with imperfect geometry based on geometric nonlinear analysis*, Comput. Meth. Appl. Mech. Engrg. 285 (2015) 452–467.
[6] M.M. Neves, H. Rodrigues and J.M. Guedes, *Generalized topology design of structures with a buckling load criterion*, Struct. Optim. 10(2) (1995) 71–78.
[7] M.M. Neves, O. Sigmund and M.P. Bendsoe, *Topology optimization of periodic microstructures with a penalization of highly localized buckling modes*, Int. J. Numerical Meth. Eng. 54(6) (2002) 809–834.
[8] J. Osher and J.A. Sethian, *Front propagating with curvature dependent speed: algorithms based on Hamilton-Jacobi formulations*, J. Comput. Phys. 79(1) (1988) 12–49.
[9] M. Otomori, T. Yamada, K. Izui and S.H. Nishiwaki, *Matlab code for a level set-based topology optimization method using a reaction diffusion equation*, Struct. Multidis. Optim. 51 (2014) 1159–1172.
[10] L. Quantian and T. Liyong, *Structural topology optimization for maximum linear buckling loads by using a moving iso-surface threshold method*, Struct. Multidis. Optim. 52(1) (2015) 71–90.
[11] J.A. Sethian and A. Wiegmann, *Structural boundary design via level set and immersed interface methods*, J. Comput. Phys. 163(2) (2000) 489–528.
[12] P. Wei, Z. Li, X. Li1 and M. Yu Wang, *An 88-line MATLAB code for the parameterized level set method based topology optimization using radial basis functions*, Struct. Multidis. Optim. 58 (2018) 831–849.
[13] Qi Xia, M. Yu Wang and Tielin Shi, *A level set method for shape and topology optimization of both structure and support of continuum structures*, Comput. Meth. Appl. Mech. Engin. 272 (2014) 340–353.
[14] Qi Xia, M. Yu Wang and Tielin Shi, *A move limit strategy for level set based structural optimization*, Engin. Optim. 45(9) (2013) 1061–1072.
[15] T. Yamada, K. Izui, S. Nishiwaki and A. Takezawa, *A topology optimization method based on the level set method incorporating a fictitious interface energy*, Comput. Meth. Appl. Mech. Eng. 199 (2010) 2876–2891.